

## Structure of inert gases from the $(e, 2e)$ reaction\*

E. Weigold, S. T. Hood, and I. E. McCarthy

*School of Physical Sciences, The Flinders University of South Australia, S. A. 5042, Australia*

(Received 21 May 1974)

The  $(e, 2e)$  reaction is used to investigate the binding energies and angular correlations for electrons ejected from the  $4p$  and  $4s$  orbitals of krypton. Configuration interaction in the ion eigenstates is the dominant feature in the ejection of a  $4s$  electron. Only  $(30 \pm 3)\%$  of the strength of the  $4s$  hole state is contained in the ion eigenstate with the dominant configuration  $4s4p^6\ ^2S_{1/2}$ . The angular correlations calculated with the distorted-wave off-shell impulse approximation, and using the Hartree-Fock wave functions of Froese-Fischer, agree very well with the observed angular correlations. In addition, relative to a  $4p^{-1}$  spectroscopic factor of unity, the  $4s^{-1}$  spectroscopic factors for the various excited ion eigenstates sum to  $0.99 \pm 0.08$ . Data are also presented on the binding energies of electrons ejected from the outer  $s$  and  $p$  orbitals in neon and argon, and the role of configuration interaction in the  $s^{-1}$  states is discussed. Incident electron energies are approximately 200, 400, and 800 eV.

### I. INTRODUCTION

In a recent series of papers we have shown that the  $(e, 2e)$  reaction can be an extremely powerful technique for studying atoms<sup>1-3</sup> and molecules.<sup>4-6</sup> In all of these experiments we used noncoplanar symmetric geometry and incident electron energies ranging from 200 eV to approximately 1 keV. We showed that the angular correlation observed when an electron is removed from the least-bound single-particle state of helium and argon can be extremely well understood in terms of the single-particle model for the atomic structure and the quantum mechanics of reactions. Outstanding features were that the shape of the angular correlation was independent of energy and directly related to the momentum wave function of the struck electron. In addition we showed that the reaction was sensitive enough to distinguish between different approximations for the wave function.

We have also used the reaction to probe the structure of eigenstates of the ion Hamiltonian other than the ground state.

A model,<sup>3</sup> similar to that of Levin,<sup>7</sup> was derived for the  $(e, 2e)$  reaction in which the differential cross section is proportional to a spectroscopic factor describing the probability of finding a particular single-hole configuration in the ion eigenstate, the shape of the cross section again being given by the distorted-wave off-shell impulse approximation.

There are therefore several criteria which the "correct" wave function must meet. Firstly, it must give the observed shape of the angular correlation. Secondly, the spectroscopic factors for a particular single-hole configuration must sum to unity over all the corresponding eigenstates. Finally, it must give the correct binding energy; the experimental position of the single-hole energy

level being defined as the centroid of all the eigenstates containing the corresponding single-hole configuration, weighted by the spectroscopic factors.

In addition to studying He and Ar, we have used the  $(e, 2e)$  reaction to study the simple diatomic molecule  $H_2$ <sup>4</sup> and the valence orbitals of the polyatomic molecule  $CH_4$ .<sup>5</sup> The results showed that the reaction probes details in molecular wave functions.

The  $(e, 2e)$  reaction has recently also been used by Van der Wiel and Brion<sup>8</sup> to investigate molecular structure. Their experimental arrangement was designed to simulate photoelectron spectroscopy by detecting fast forward-scattered electrons in coincidence with slow electrons ejected at  $90^\circ$ . Although this technique does not allow the determination of electron momentum distributions, it has several advantages over photoelectron spectroscopy. Other electron-electron coincidence experiments by Camilloni *et al.*<sup>9</sup> and by Ehrhardt *et al.*<sup>10</sup> were concerned with inner-shell structure and with angular correlations at very low ejected energies, respectively. The electron momentum distribution in atoms, molecules, and solids has recently been extensively investigated using Compton scattering of x rays<sup>11</sup> and  $\gamma$  rays,<sup>12</sup> inelastic scattering of high-energy electrons,<sup>13</sup> and positron annihilation.<sup>14</sup>

The last method requires a knowledge of the positron wave function in the target, which depends on the charge distribution, so that at best a "self-consistent" approach is possible. All these techniques fail to distinguish different final states of the ion, though in a recent experiment<sup>15</sup> the  $1s$  shell was isolated by detecting the scattering photon in coincidence with a fluorescence x ray. The results did not agree with the predictions of the impulse approximation; so no structural information was obtained. The "Compton profiles" provided by all these techniques require differentiation of the ex-

perimental data to yield the radial momentum distribution, which considerably degrades the accuracy obtained.

The purpose of the present work is to extend our earlier measurements on helium and argon to other inert gases, and in particular to investigate the role of configuration interaction resulting from electron correlation effects in the hole states in the valence  $s$  shells.

## II. APPARATUS

The experimental apparatus has been described only briefly in earlier publications, and therefore a more extensive description will be given here. The vacuum chamber consisted of a stainless-steel cylinder, 76.1 cm high and 54.5 cm in internal diameter, sealed at the top and bottom to aluminium plates by means of O rings. The chamber was pumped by a 6-in. mercury diffusion pump and associated liquid-nitrogen trap through a port in the bottom plate. The experimental apparatus shown in Fig. 1 was mounted on this plate. Base pressures of  $8 \times 10^{-7}$  Torr were obtained with the experiments conducted in a dynamic chamber pressure of about  $10^{-5}$  Torr. The pressure in the interaction region was generally an order of magnitude or so higher than this. Long term stability of the background pressure was about 5%.

Target gases were of at least 99.9% purity and were held in one or more glass reservoirs of 1-l capacity at pressures of several hundred Torr. Gas was admitted to the vacuum chamber by a leak valve through a cold trap and a length of tubing, which terminated within a few millimeters of the electron beam in a capillary tube of 0.025-cm i.d. Calculation of the gas throughput at the normal pressure showed that the flow through the capillary was not effusive. The pumping speed in the interaction region was limited by the tube holding the inner slit system (Fig. 1), so that the gas density varied only slowly with position near the capillary orifice. A set of deflection plates was used to align the electron beam from a commercial electron gun with a Faraday cup whose entrance aperture was 0.125 cm. The beam was focused by maximizing the ratio of the current into the cup to the spray current collected on the front face. This ratio was generally of the order of  $10^3$ . Beam currents varied with the energy and the age of the gun from over 100 to less than  $10 \mu\text{A}$ .

Two electron-energy analyzers were required to define the energies and directions of the emitted electrons. From the many designs available in the literature,<sup>16</sup> the cylindrical-mirror analyzer<sup>17</sup> was chosen because of its simple construction, high-resolution, and superior electron optical proper-

ties. The choice of symmetric noncoplanar scattering geometry (i.e., azimuthal angular variation) as opposed to the more usually discussed symmetric coplanar situation was made on several grounds. Firstly, because of the cylindrical symmetry only the entrance aperture of one analyzer had to be moved in the azimuthal direction. This made the mechanical arrangement simple and compact. Secondly, the interaction volume should be independent of angle if the width of the electron beam is kept smaller than the viewing angles of the two spectrometers. This could only be arranged in the coplanar system by using a well-collimated target beam with a consequent loss of intensity. Thirdly, the singles counting rates and angular correlation obtained must be symmetric about  $\phi = 0$ , providing a check on instrumental distortions. Further, the angular correlations are proportional to the momentum distribution alone, since the off-shell Coulomb  $T$  matrix<sup>2</sup> is independent of  $\phi$ . In practice, the count rate of the fixed analyzer was used to monitor the product of beam current and gas density, while the count rate of the movable analyzer was used to correct for any angular variation of sensitivity.

The two analyzers were of similar construction and were mounted on opposite sides of a vertical aluminium plate which was cut out in the center to carry the electron gun, deflection plates, and Faraday cup. The axes of the analyzers were coincident with the electron beam. Each analyzer consisted of an inner half cylinder machined from stainless steel with an outer plate rolled from stainless sheet supported by Teflon end plates. Fringing fields were minimized by attaching stainless-steel annular segments to the end plates and connecting them by stainless-steel rods along the edge of the analyzer. The rings were connected by a resistor chain between the negative outer plate and the grounded inner plate. The azimuthal angle enclosed was  $150^\circ$  in both cases, compared with the range  $-40^\circ \leq \phi \leq +40^\circ$  over which data were taken. The entrance and exit slits were sufficiently far from the end plates so that the fringing fields were negligible.

Both entrance and exit apertures on the fixed analyzer were holes drilled in tantalum foil at an angle of  $45^\circ$  to subtend  $5^\circ$  along both diameters at the source and detector, respectively. The exit aperture on the other analyzer was a slit subtending  $5^\circ$  at the detector while the entrance aperture was another  $5^\circ$  hole drilled in a long tantalum strip running around the inner plate and over rollers. The ends were attached to either end of a miniature chain running over a sprocket on a rotary feed through. Rotation of the shaft thus changed the acceptance angle of this analyzer. The electron de-

tectors were Mullard channel-electron multipliers (CEM), which were mounted in silicone gel inside small aluminium boxes fitted with variable apertures. They were mounted with their apertures on an axis orientated at  $45^\circ$ . The CEM on the movable analyzer was rotated in unison with the entrance slit by a second chain drive. The source size for both analyzers was defined in the radial direction by the electron beam ( $\sim 1$  mm) and in the axial direction by a pair of slits mounted on a copper tube of 12-mm internal diameter surrounding the beam as shown in Fig. 1. This figure also shows the dimensions of the two analyzers.

The expression for the resolution of each analyzer for the configuration used in this work was dominated by the term due to the axial extent of the source and detector. The important quantity was the FWHM of the resolution function obtained in coincidence experiments, which was a convolution of the two analyzer functions and the energy distribution of the electron beam; for the combination of slit sizes used in the present work this resolution

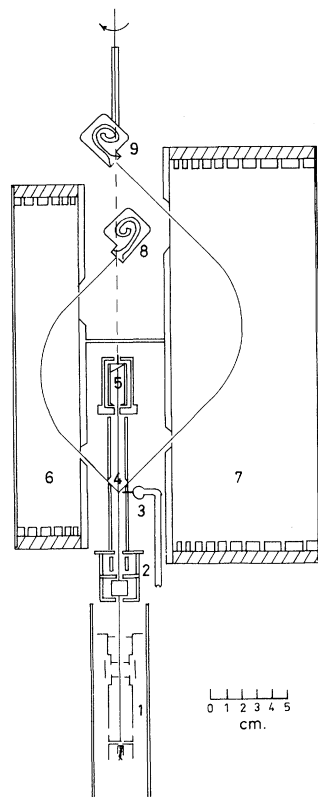


FIG. 1. Schematic diagram of the experimental apparatus: 1: electron gun; 2: deflection assembly; 3: gas inlet; 4: inner-slit assembly; 5: Faraday cup; 6: fixed analyzer; 7: movable analyzer; 8: fixed CEM; 9: movable CEM.

was 1.2% of the summed final energies. The binding-energy scale was calibrated directly by using a gas such as helium, which could be mixed with the gas under study, to obviate problems associated with space charge and contact potentials. The vacuum chamber was lined with mu-metal and surrounded by a pair of Helmholtz coils giving fields less than 5 mG within the analyzers. All exposed surfaces were coated with colloidal graphite to reduce stray fields. The entrance cones of the CEM's were biased up to 50 V negative to repel low-energy electrons.

The signal processing electronics have been discussed in earlier publications.<sup>1,2</sup> In brief, pulses from the CEM's were amplified by preamplifiers and double delay line amplifiers. Two fast timing discriminators were triggered in the zero-crossing mode. The output from one timing discriminator provided a stop pulse. The output spectrum from the time-to-amplitude converter was fed to a multi-channel analyzer, which was used to set up the experiment and to monitor the time resolution. A typical time delay spectrum is shown in Fig. 2, where the resolving time is 10 nsec at 0.1 maximum. Two single-channel analyzers were set up to accept events in the ranges shown in Fig. 2. If the "background" single-channel analyzer window is set  $x$  times broader than the window set over the coincidence peak, the true coincidence rate is given by  $T = C - B/x$ , and the standard deviation by  $\sigma_T = (C + B/x^2)^{1/2}$ .  $C$  and  $B$  are the counts registered in a given time by scalars looking at the "coincidence" and background windows, respectively. The advantage of using large values of  $x$  for cases where the true rate is small is obvious. In the present work  $x$  was set equal to 4.

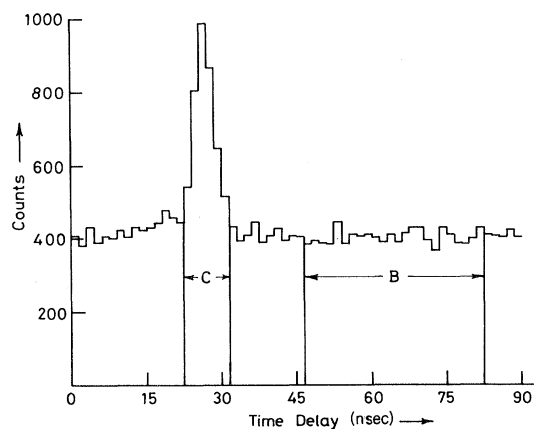


FIG. 2. Typical time-delay spectrum showing window settings.

### III. DETERMINATION OF SPECTROSCOPIC FACTORS

The theory of the determination of spectroscopic factors was given in some detail in Ref. 3. Since the main atomic-structure effect observed in the present experiments is the excitation of different eigenstates of the same total angular momentum and parity, we will concentrate on this aspect and assume that the initial atom does not have significant ground-state correlations. (The effect of ground-state correlations has been demonstrated<sup>27</sup> for the case of helium in another publication.)

In the notation of Ref. 3, the atomic eigenstate  $\Psi_0$  is assumed to be the ground-state Hartree-Fock configuration  $\Phi_0(0)$ . The ion eigenstate is a linear combination of independent-particle configurations  $\Phi'_\sigma(\beta)$ :

$$\Psi'_0 = \sum_{\beta} b_{\sigma}(\beta) \Phi'_{\sigma}(\beta), \quad (1)$$

where primed wave functions denote a  $(Z-1)$ -particle system. Denoting the coordinates of the incident and ejected electrons (for which antisymmetry is eventually imposed) by 0 and 1, the ( $e, 2e$ ) amplitude for excitation of an ion state of total angular-momentum quantum numbers  $J$ ,  $m$  and parity  $\pi$  is equal (apart from constant kinematic factors) to

$$M_{J\pi}^m = \langle \Psi_{\text{total}}^{(-)}(\vec{k}_A, \vec{k}_B) | V_0 + V_{01} | \vec{k}_0, \Psi_0 \rangle. \quad (2)$$

In Ref. 3 we made the optical-model approximation for  $\Psi_{\text{total}}^{(-)}$ , in the case where the state  $\sigma$  of the ion is excited:

$$\Psi_{\text{total}}^{(-)}(\vec{k}_A, \vec{k}_B) = u_{\sigma}^{(-)}(\vec{k}_A, \vec{k}_B) \Psi'_{\sigma}. \quad (3)$$

This approximation assumes that the ion state  $\Psi'_{\sigma}$  consists of the original atomic state  $\Psi_0$  (called the unexcited core) coupled to hole state  $\psi_{\rho}(\vec{k}_1)$ , where the single-particle quantum numbers  $\sigma$  account for  $J$ ,  $m$ , and  $\pi$ . This ion configuration is denoted  $\Phi'_\sigma(0)$ . The two final-state electrons merely scatter elastically from the core. Inelastic scatterings, corresponding to the core-excited configuration  $\Phi'_\sigma(\beta)$  for  $\beta \neq 0$ , are simply included in a complex term in the potential, in which the two-electron continuum function  $u_{\sigma}^{(-)}$  is computed.

The present work shows that some ion states have quite small spectroscopic factors (of order 0.3 or less), so that core-excited configurations play a large part in the expansion (1) of the ion eigenstate. It therefore seems inconsistent not to include explicitly the parts of the amplitude involving such configurations. A detailed discussion of this point will be deferred to a future publication. We will, however, explain why the determination of spectroscopic factors is not invalidated by core excitations.

Each core-excited configuration is denoted by

$$\Phi'_{\sigma}(\beta) = [\psi_{\rho} \times \Psi_{\beta}]_{\sigma}, \quad (4)$$

where the single-particle angular momenta  $\rho$  couple to the excited-core angular momenta  $\beta$  to give the ion quantum numbers  $\sigma$ . In the specific cases of  $\frac{1}{2}+$  ion eigenstates considered here, shell models such as that of Luyken<sup>25</sup> depend only on the  $0+$  core ground state and  $2+$  core-excited states, so that the corresponding particle states  $\psi_{\rho}$  are  $s-$  and  $d-$ states, respectively:

$$M_{\sigma} = \sum_{\beta} b_{\sigma}(\beta) \times \langle u_{\sigma}^{(-)}(\vec{k}_A, \vec{k}_B) | [\psi_{\rho} \times \Psi_{\beta}]_{\sigma} | V_0 + V_{01} | \vec{k}_0, \Psi_0 \rangle. \quad (5)$$

The parts of this amplitude that do not depend on the core coordinates constitute the amplitude of Ref. 3. This is a three-body amplitude, evaluated by the distorted-wave off-shell impulse approximation of Ref. 2, multiplied by a spectroscopic amplitude  $b_{\sigma}(0)$ , whose square is the spectroscopic factor  $S_{\sigma}(0)$ . This approximation includes the diagonal matrix element of the optical-model potential  $\langle \Psi_0 | V_0 | \Psi_0 \rangle$  by transforming to a distorted wave  $\chi_0(\vec{k}_0)$ . It is calculated in the present work.

In order to allow for explicit core-excited terms we must keep the off-diagonal optical-model terms

$$v_{\beta 0} = \langle \Psi_{\beta} | V_0 | \Psi_0 \rangle. \quad (6)$$

In addition to the leading term used in the present work, we have terms for each core-excited configuration  $\beta$  of the form

$$b_{\sigma}(\beta) \langle u_{\sigma}^{(-)}(\vec{k}_A, \vec{k}_B) | [\psi_{\rho}^{\dagger} \times v_{\beta 0}]_{\sigma} | \chi_0(\vec{k}_0) \rangle. \quad (7)$$

It is immediately obvious that such terms are small, not only because of the rather small structure amplitudes  $b_{\sigma}(\beta)$ , which may also be small in the leading term, but also because of the core-excitation amplitudes  $v_{\beta 0}$ . These amplitudes are responsible for inelastic scattering from the atomic core, which is well known to be small compared to elastic scattering. The elastic amplitude, like the leading ( $e, 2e$ ) term, is of zeroth order in  $v_{\beta 0}$ .

It is not necessary to perform an explicit calculation of the terms of order  $v_{\beta 0}$  (although one is currently being performed) in order to test the validity of the use of the leading term in the determination of spectroscopic factors. Such terms have an entirely different structure from the leading term. In particular, they are strongly energy dependent and state dependent, whereas the shape of the leading term is independent of energy in the present noncoplanar symmetric geometry, and, of course, includes only the unexcited core state. The leading term is therefore seen experimentally to be a valid approximation in kinematic regions

where the cross-section shape is energy independent and state independent. For argon and krypton this appears to be the case for momentum transfers less than about  $1a_0^{-1}$ , within the present experimental accuracy. Error in making this assumption is included in the error involved in the satisfaction of the sum rule for spectroscopic factors,

$$\sum_{\sigma} S_{\sigma}(0) = 1. \quad (8)$$

If the sum rule is satisfied within experimental error, this lends plausibility to the assumption that the core-excitation contribution to the amplitude is small at momentum transfers for which relative magnitudes of  $s^{-1}$  angular correlations are compared.

The procedure for evaluating spectroscopic factors is therefore as follows:

(i) Measure the binding-energy spectra at various fixed angles (i.e.,  $q$ ) by varying the incident energy for a given final energy.

(ii) Identify the total angular momentum and parity of the ion states by the angular correlation shape. This is obtained by varying the angle and keeping the incident and final energies fixed. In the present cases spin-orbit splitting is not resolved and we denote different types of state by  $s^{-1}$  and  $p^{-1}$ .

(iii) If there is only one state of a given type, its spectroscopic factor is assumed to be 1. If the angular correlation is given to a good approximation by the three-body cross section of Ref. 2 using an approximate Hartree-Fock wave function, this is regarded as confirmation of this assumption. Such is the case for  $p^{-1}$  states in neon, argon, and krypton.

(iv) If there is more than one state of a certain type (as there is for  $s^{-1}$  states in argon and krypton, but not neon) the angular correlations are compared with the three-body calculation of Ref. 2 using an approximate Hartree-Fock wave function. In the momentum-transfer region where angular correlations in noncoplanar symmetric geometry are energy and state independent, the assumption that the angular correlation is proportional to the spectroscopic factor is assumed to be valid.

(v) Spectroscopic factors are evaluated by comparing experimental cross sections  $\sigma(q)$  using three-body amplitudes  $T_{\sigma}$ . The ratio of cross sections at given momentum transfer for  $s^{-1}$  and  $p^{-1}$  states is

$$\frac{\sigma_s(q_1)}{\sigma_p(q_2)} = \frac{\sum_{J_s} (2J_s + 1)^2 |T_s(q_1)|^2 S_s}{\sum_{J_p} (2J_p + 1)^2 |T_p(q_2)|^2 S_p} = \frac{4}{20} \frac{|T_s(q_1)|^2 S_s}{|T_p(q_2)|^2 S_p}$$

(vi) In the present cases, since we know  $S_p = 1$ ,

we may calculate  $S_s$  absolutely for each  $s^{-1}$  state, even though there is one arbitrary factor multiplying all the experimental data.

(vii) The spectroscopic factors for a particular type of state (e.g.,  $s^{-1}$ ) are summed. If their sum is unity, this is regarded as a check of the validity of the theory as well as of the assumption that no states have been missed in the experiment.

#### IV. RESULTS AND DISCUSSION

If the target atom is considered to be at rest, then the momentum transfer to the residual ion in the  $(e, 2e)$  reaction is given by  $\vec{q} = \vec{k}_A + \vec{k}_B - \vec{k}_0$ , where the subscript 0 refers to the incident electron and the subscripts A and B to the two outgoing electrons. In the symmetric noncoplanar geometry both electrons are emitted at equal angles to the incident direction ( $45^\circ$  in the present case), and both are selected to have the same energy ( $E_A = E_B$ ). Then the magnitude of the momentum transfer is given by

$$q = |(2k_A \cos \theta - k_0)^2 + 4k_A^2 \sin^2 \theta \sin^2 \frac{1}{2} \phi|^{1/2}.$$

Neglecting the recoil energy of the ion because of its large mass, the incident electron energy  $E_0$  can be simply related to the binding energy or separation energy  $\epsilon$  of the ejected electron and the total energy  $E = E_A + E_B$  of the emitted electrons by  $E_0 = \epsilon + E$ .

Figures 3 and 4 show the variation of coincidence

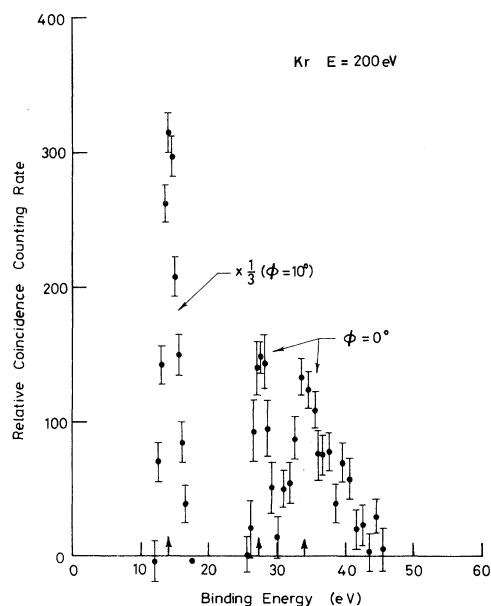


FIG. 3. Variation of the coincidence counting rate with binding energy for krypton at a total electron energy  $E$  of 200 eV. Arrow at  $\epsilon = 34$  eV indicates the position of the  $4s^2 4p^4 4d^2 S_{1/2}$  ion eigenstate.

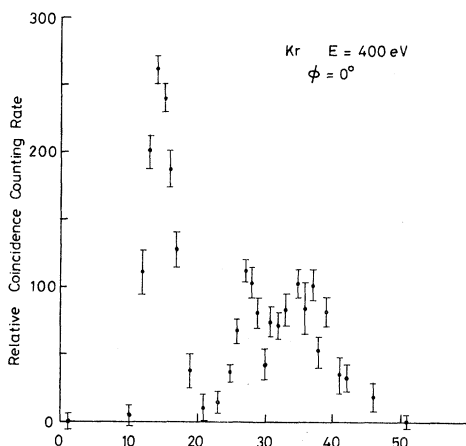


FIG. 4. Variation of coincidence counting rate with binding energy for krypton obtained with  $E=400$  eV.

counting rate observed for krypton when the incident energy  $E_0$  is varied and the total energy  $E$  is kept constant at 200 and 400 eV, respectively. The peak at 14.1 eV corresponds to the ejection of a  $4p$  electron leaving the ion in its ground state with the configuration of  $4s^2 4p^5$ . The peak at 27.4 eV results from a transition leaving the ion in its first excited state. This state of the ion has traditionally been identified with the  $4s$  hole state, that is, the configuration  $4s^1 4p^6$ . Further transitions can be seen leaving the ion in higher excited states and even in the continuum, which begins at  $\epsilon = 38.6$  eV. Such transitions can be produced by a number of mechanisms. The angular correlations to be discussed later show that only direct mechanisms need be considered.<sup>1</sup> We have previously discussed<sup>3</sup> the dominant effect of final-state configuration interaction in the electron-impact ionization of argon using the distorted-wave off-shell impulse approximation. This previous discussion did not include the possibility of nonorthogonality between atomic and ionic basis functions due to the different self-consistent potentials. Effects of nonorthogonality have sometimes been called shake up and shake off. The functions of  $Z-1$  particles which appear in the fractional parentage expansion of the atom<sup>3</sup> thus overlap with more than one configuration constructed from single-particle states calculated in the ion self-consistent potential. Our previous derivation can be generalized to include this effect by expanding the final ion states  $\Psi'_\sigma$  in configurations  $\Phi'_\sigma(\beta)$  constructed from atomic single-particle states,

$$\Psi'_\sigma = \sum_{\beta} b_{\sigma}(\beta) \Phi'_\sigma(\beta),$$

where now the amplitudes for one-particle, one-hole excitations need not be zero. The cross sec-

tion will, as before, be proportional to the spectroscopic factor  $|b_{\sigma}(0)|^2$ , but, of course, additional states  $\sigma$  of the same angular momentum and symmetry may contain the single-hole configuration under consideration. The assignment of ion eigenstates to either configuration interaction or electron shake up (off) depends on the choice of basis.

Calculations by Carlson and Nestor<sup>18</sup> of the total probability for shake up and shake off indicate that this probability is small for the ejection of electrons from outer shells, thus showing that the effects of nonorthogonality are unimportant. The calculations, based on relativistic Hartree-Fock-Slater wave functions, give a value of approximately 4% for the total probability of shake up and shake off when an electron is ejected from the  $4s$  orbital of krypton. This is negligible compared to the observed probability shown in Figs. 3 and 4 for transitions leading to the higher excited states. The probability for transitions leading to the first excited state of Kr II with  $\epsilon = 27.4$  eV relative to that for all excited states ( $\epsilon \geq 27.4$  eV) is  $0.29 \pm 0.04$  at 200 eV and  $0.31 \pm 0.04$  at 400 eV. Figures 3 and 4 also show that although the contribution with separation energy above 27.4 eV has a well-defined peak at approximately 34–35 eV, the peak is too broad to be accounted for by the excitation of a single state.

Figures 5 and 6 show the angular correlations obtained for electrons with separation energies of 27.4 and 37 eV, respectively. The correlations, for total energies of 400 and 800 eV, are plotted as a function of the momentum transfer  $q$ . In agreement with our earlier results on helium and

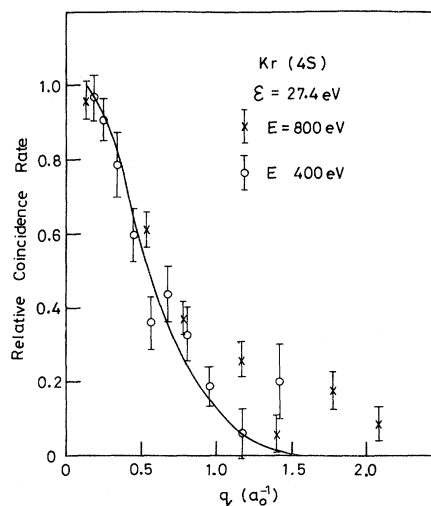


FIG. 5. Angular correlation observed for the ejection of electrons from krypton with binding energy of 27.4 eV compared with that predicted by the  $4s$  krypton wave function of Froese-Fischer (Ref. 19).

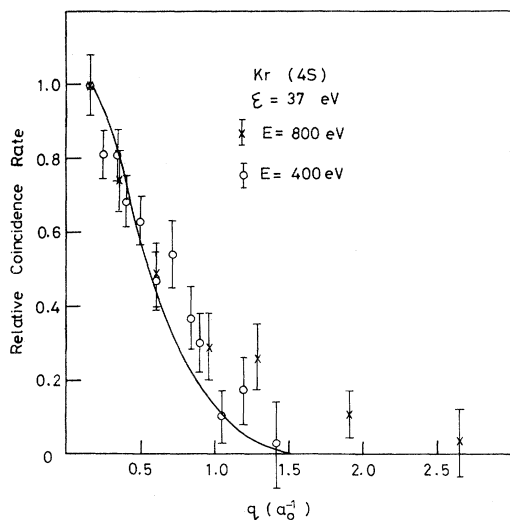


FIG. 6. Angular correlation observed for the ejection of electrons from krypton with binding energy of 37 eV compared with that predicted by the 4s krypton wave function of Froese-Fischer (Ref. 19).

argon, the angular correlations are observed to be independent of the energy  $E$  and depend only on the momentum transfer  $q$ . The solid line in the figures is the angular correlation calculated using the distorted-wave off-shell impulse approximation<sup>2,3</sup> with low distortion. In effect, the curve is the square of the momentum-space wave function of an electron in the 4s subshell of krypton. The wave function used was the Hartree-Fock wave function of Froese-Fischer.<sup>19</sup> The two angular correlations are strikingly similar and both can be fitted extremely well with the 4s momentum-density distribution, except perhaps at large momentum transfers where the experimental errors are large.

The two peaks with higher separation energies must both therefore correspond to the ejection of a 4s electron from krypton. The strength of the 4s hole state in Kr is therefore severely split among a number of ion eigenstates, only 30% of the strength being in the first excited state of the ion, normally given the ion configuration  $4s4p^6$ . In other words there must be a large amount of configuration interaction in the ion eigenstates as a result of electron-electron correlations.

Since the binding energy of the single-hole energy level is defined<sup>3,20</sup> to be the centroid of all the eigenstates containing the single-hole configuration weighted by the spectroscopic factors, the binding energy of the 4s hole state is not 27.4 eV. Analysis of the data in Figs. 3 and 4 yields a binding energy of  $33.4 \pm 0.7$  eV. This can be compared with the value of 32.1 eV obtained from the Hartree-Fock calculations of Froese-Fischer. Inclusion of relativistic effects would lead to an increase in the

binding energy of approximately 2 eV.<sup>21</sup>

The possible importance of configuration interaction in the single ionization of krypton by the ejection of a 4s electron was pointed out by Luyken *et al.*<sup>22</sup> They came to this conclusion as a result of an optical study of the excitation of the  $4s4p^6^2S_{1/2}$  ionic level in krypton by electron impact, although no numerical data stood at their disposal.

The configuration interaction first observed by us<sup>1,3</sup> in electron-impact ionization should also be observable in photoionization of the s subshell. Recently such data on inert gases have been reported by Spears *et al.*,<sup>23</sup> who used the x-ray photoelectron spectroscopy technique. They observed some satellite structure and assigned approximately 20% of the strength of the  $4s^{-1}$  state to an ion eigenstate at  $\epsilon = 34$  eV, with the suggested designation<sup>24</sup> of  $4s^24p^4(^1D)4d^2S_{1/2}$ . In addition to a small contribution assigned to shake up accompanying 4p ionization, some higher structure was observed but was not discussed by them. The  $4s^24p^4d^2S_{1/2}$  state, indicated by an arrow in Fig. 3, must arise through configuration interaction in either the atom or the ion.<sup>3,7</sup> The angular correlation in Fig. 6 shows that the configuration interaction is in the ion, since it has the shape characteristic of the 4s hole rather than the 4d hole. This is in agreement with the conclusion of Minnhagen *et al.*,<sup>24</sup> who found a strong interaction between the  $sp^6^2S_{1/2}$  and  $(^1D)4d^2S_{1/2}$  levels.

The present results for krypton can be compared with our earlier results for argon,<sup>1,3</sup> which were also interpreted as resulting from configuration interaction in the ion eigenstates. Figure 7 shows the binding energy spectrum for argon obtained at a total energy of 200 eV. The shape and size of the high-energy peak interpreted as being due to configuration interaction in the ion is in agreement with the earlier data taken by us at higher energy with poorer resolution. The strength of the 3s argon hole state is divided between the  $3s3p^6$  ion eigenstate and one or two higher excited states which have a total contribution of  $42 \pm 4\%$ . As discussed in detail earlier,<sup>1,3</sup> this is in agreement with a configuration interaction calculation by Luyken,<sup>25</sup> who concluded that the 3s argon hole state should be split primarily between the three ion eigenstates  $3s3p^6^2S_{1/2}$ ,  $3s^23p^4^3d^2S_{1/2}$ , and  $3s^23p^4^4d^2S_{1/2}$ , in the ratios 0.62:0.31:0.07. The position and shape of the high-energy peak in Fig. 7 is consistent with the major contribution arising from the  $3s^23p^4^3d^2S_{1/2}$  state with a separation energy of 38.6 eV, and a much smaller contribution from the  $3s^23p^4^4d^2S_{1/2}$  state at 41.2 eV. If the configuration interaction occurred in the atom rather than the ion, i.e., if the high-energy peak was due to the knock out of d-state electrons from argon  $3s^23p^4nd^2$  configura-

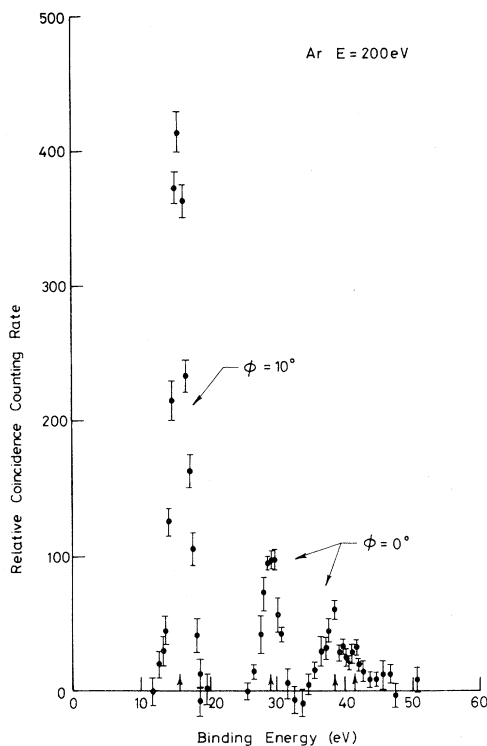


FIG. 7. Coincidence counting rate vs binding energy for argon with  $E=200$  eV. Arrows indicate the positions of the various ion eigenstates discussed in the text.

tions, the angular correlation should not peak at  $q=0$  as observed, but should be given by the square of the  $nd$  momentum-space wave function.<sup>7</sup>

The recently reported photoionization data of Spears *et al.*<sup>23</sup> on argon show some structure at an energy corresponding to the final ion eigenstates discussed above and a very small contribution due to shake up. There is, however, again a discrepancy between the photoionization results and the present data. The role of configuration interaction is much less significant in the photoionization data than in the  $(e, 2e)$  results. There is an independent check on the strengths of excited states, these being proportional to the spectroscopic factors which must sum to unity. In the case of  $(e, 2e)$  on argon the  $3s^{-1}$  spectroscopic factors do indeed sum to unity within experimental error.<sup>3</sup>

Figure 8 shows the binding or separation energy spectrum obtained for neon at a total energy of 400 eV. The two peaks at 21.6 and 48.5 eV correspond to the ejection of a  $2p$  and a  $2s$  electron leaving the ion in its ground state ( $2s^2 2p^5$ ) and first excited states ( $2s 2p^6$ ), respectively. In contrast to the Ar and Kr results, the absence of any contributions with separation energies above 48.5 eV shows that configuration interaction plays an insignificant

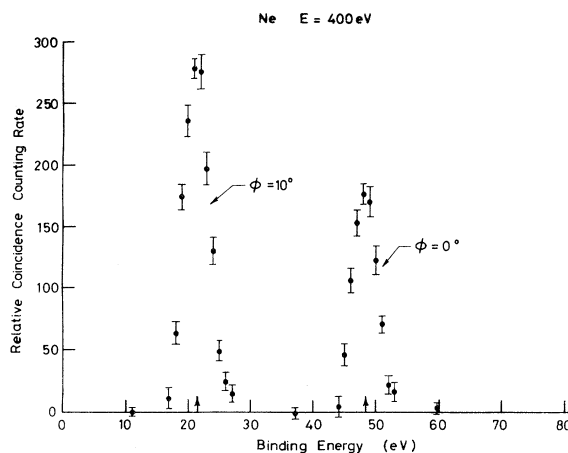


FIG. 8. Coincidence counting rate vs binding energy for neon with  $E=400$  eV.

role in the  $2s$  hole state of neon. This is also in agreement with Luyken's wave-function expansions, which gave 99% of the strength of the  $2s$  hole state to the  $2s 2p^{6,2} S_{1/2}$  ion eigenvector component. Since the configuration interaction in the argon ion is primarily due to  $d$  orbitals, and that in the krypton ion can be given a similar tentative assignment,<sup>24</sup> the absence of  $d$  orbitals in the  $n=2$  shell would explain the minor role of configuration interaction in neon. In Luyken's neon wave-function expansion, what little configuration interaction there is is contributed by the  $2s^2 2p^4 3d$  component (with  $\epsilon=60$  eV). The important role of the  $d$  orbital in the electron correlation effect observed in valence  $s^{-1}$  (hole) states of the inert gases may result from quadrupole collective excitations in the core, which cannot occur without exciting electrons into  $d$  states. Further evidence for this comes from the argon shell-model calculation of Luyken,<sup>25</sup> which is confirmed by the  $(e, 2e)$  experiment.<sup>3</sup> Each of Luyken's eigenvectors for the three observed states with spin and parity  $\frac{1}{2}+$  have large coefficients only for configurations with excited core spin and parity  $2+(^1D)$ . Those excited configurations with core spin and parity  $0+(^1S)$  are suppressed.

The angular correlation for the ejection of the outer  $p$  orbital from krypton is shown in Fig. 9. Owing to the finite angular resolution of the apparatus ( $8^\circ$ ), the coincidence counting rate does not drop to zero at  $q=0$ , as expected for a  $p^{-1}$  state. This effect is more pronounced at 800 eV since the angular range of the correlation becomes more restricted at higher energies. The two curves in the figure have been calculated using the  $4p^{-1}$  krypton wave function of Froese-Fischer. Agreement between theory and experiment is very good.

The relative magnitudes of differential cross sections for excitations of different ion eigenstates



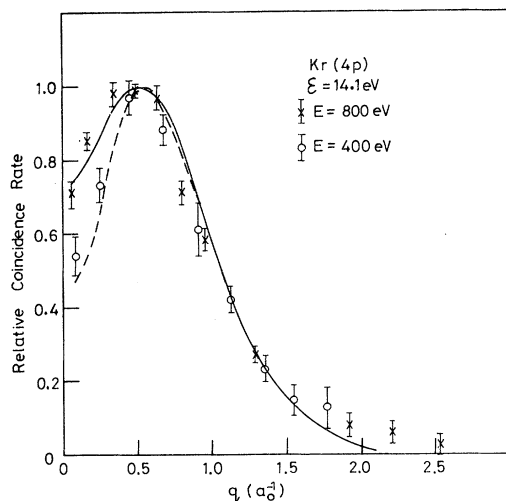


FIG. 9. Angular correlation observed for the ejection of electrons from krypton with binding energy of 14.1 eV compared with that predicted by the  $4p$  wave function of Froese-Fischer (Ref. 19). Solid curve, calculated at  $E=800$  eV; dashed curve, at  $E=400$  eV. The experimental angular resolution has been folded into the calculation.

have also been measured in the experiment. Cross sections for ion eigenstates of the same total angular momentum and parity are proportional to the probability of finding the appropriate single-hole configuration in the eigenstate. They can also be compared with cross sections for ion eigenstates of different total angular momentum, as discussed in Sec. III.

We assume that the wave function of the ground state of the krypton ion consists purely of the configuration  $4p^{-1}$ . This is supported by the fact that only one energy level with a  $4p^{-1}$  angular correlation is observed. In addition, in order to determine meaningful spectroscopic factors we must use a reaction model and a single-particle model for the atom that adequately reproduces the angular correlation shape. The Hartree-Fock model of Froese-Fischer gave, in the distorted-wave off-shell impulse approximation, theoretical curves which fit the  $4p^{-1}$  and  $4s^{-1}$  data very well for all but the highest measured momentum-transfer values.

In order to compare relative magnitudes of cross sections we have chosen to consider  $4s^{-1}$  angular correlations at minimum momentum transfer ( $\phi = 0$ ) and  $4p^{-1}$  angular correlation at  $q = 0.46a_0^{-1}$ . These points are both in the region where the shape

is excellently reproduced by the model, and they are near maxima, so that the effect of folding in the experimental acceptance angle is minimized.

The sum of the  $4s^{-1}$  spectroscopic factors for the various excited ion eigenstates is  $0.99 \pm 0.08$  for the Hartree-Fock wave function of Froese-Fischer. Within experimental error it therefore satisfies the rule that the sum of the spectroscopic factors for all ion eigenstates contained in a given hole state should be unity.

## V. SUMMARY AND CONCLUSIONS

The experimental angular correlations obtained in the  $(e, 2e)$  reaction on krypton using the symmetric noncoplanar geometry are very well described by the distorted-wave off-shell impulse approximation and the Hartree-Fock wave functions of Froese-Fischer.

The experimental angular correlations and separation-energy spectra show that although there is very little, if any, configuration interaction in the  $4p^{-1}$  state; many ion eigenstates contain the  $4s^{-1}$  configuration. In fact, configuration interaction is no longer a small effect, but is dominant, only 30% of the  $4s^{-1}$  configuration being contained in the first excited state of the ion. The experimental position of the single-hole energy level, defined to be the centroid of all ion eigenstates containing the corresponding single-hole configuration weighted by the spectroscopic factors, is therefore considerably different from that established by photoelectron spectra such as those reported by Siegbahn *et al.*<sup>26</sup> It is shifted from 27.4 to 33.4 eV, slightly higher than the  $4s^{-1}$  energy level determined by the Hartree-Fock theory of Froese-Fischer.

In contrast with the results for krypton, configuration interaction is not significant in the  $2s^{-1}$  configuration of neon. However, it is quite significant in the  $3s^{-1}$  configuration of argon. The  $(e, 2e)$  reaction therefore provides an important tool for investigating electron correlation in atoms and ions.

Another criterion, which depends both on the validity of the reaction model and the single-particle model of the atom, is that the spectroscopic factors should sum to unity. The spectroscopic factors for  $4s^{-1}$  configurations in the various krypton ion eigenstates observed to have the  $4s^{-1}$  angular correlation shape are determined relative to the ground state, which is assumed to be 1 since only one such eigenstate is observed. Their sum is 1 within experimental error.

- \*Supported in part by the Australian Research Grants Committee.
- <sup>1</sup>E. Weigold, S. T. Hood, and P. J. O. Teubner, *Phys. Rev. Lett.* **30**, 475 (1973).
- <sup>2</sup>S. T. Hood, I. E. McCarthy, P. J. O. Teubner, and E. Weigold, *Phys. Rev. A* **8**, 2494 (1973).
- <sup>3</sup>S. T. Hood, I. E. McCarthy, P. J. O. Teubner, and E. Weigold, *Phys. Rev. A* **9**, 260 (1974).
- <sup>4</sup>E. Weigold, S. T. Hood, I. E. McCarthy, and P. J. O. Teubner, *Phys. Lett. A* **44**, 531 (1973).
- <sup>5</sup>S. T. Hood, E. Weigold, I. E. McCarthy, and P. J. O. Teubner, *Nature* **245**, 65 (1973).
- <sup>6</sup>I. E. McCarthy, *J. Phys. B* **6**, 2358 (1973).
- <sup>7</sup>V. G. Levin, *Phys. Lett. A* **39**, 125 (1973).
- <sup>8</sup>M. J. Van der Wiel and C. E. Brion, *J. Electron Spectrosc.* **1**, 309 (1973).
- <sup>9</sup>R. Camilloni, A. Giordini Guidoni, R. Tiribelli, and G. Stefani, *Phys. Rev. Lett.* **29**, 618 (1972).
- <sup>10</sup>H. Ehrhardt, M. Schulz, T. Tekaat, and K. Willmann, *Phys. Rev. Lett.* **22**, 89 (1969); H. Ehrhardt, K. H. Hesselbacher, K. Jung, and K. Willmann, *J. Phys. B* **5**, 1559 (1972).
- <sup>11</sup>M. Cooper, *Adv. Phys.* **20**, 453 (1971); I. R. Epstein, *Acc. Chem. Res.* **6**, 145 (1973).
- <sup>12</sup>P. Eisenberger and W. A. Reed, *Phys. Rev. A* **5**, 2085 (1972).
- <sup>13</sup>H. F. Wellenstein and R. A. Bonham, *Phys. Rev. A* **7**, 1568 (1973).
- <sup>14</sup>R. N. West, *Adv. Phys.* **22**, 263 (1973).
- <sup>15</sup>T. Fukamachi and S. Hosoya, *Phys. Lett. A* **38**, 341 (1972).
- <sup>16</sup>W. Steckelmacher, *J. Phys. E* **6**, 1061 (1973).
- <sup>17</sup>V. V. Zashkvara, M. I. Korsyskii, and O. S. Kosmachev, *Zh. Tekh. Fiz.* **36**, 132 (1966) [*Sov. Phys.—Tech. Phys.* **11**, 96 (1966)]; H. Z. Sar-el, *Rev. Sci. Instrum.* **38**, 1210 (1967); S. Aksela, M. Karras, M. Pessa, and E. Suoninen, *Rev. Sci. Instrum.* **41**, 351 (1970); J. S. Risley, *Rev. Sci. Instrum.* **43**, 95 (1972).
- <sup>18</sup>T. A. Carlson and C. W. Nestor, Jr., *Phys. Rev. A* **8**, 2887 (1973).
- <sup>19</sup>C. Froese-Fischer, *At. Data* **4**, 301 (1972).
- <sup>20</sup>R. Manne and T. Aberg, *Chem. Phys. Lett.* **7**, 282 (1970); H. W. Meldner and J. D. Perez, *Phys. Rev. A* **4**, 1388 (1971).
- <sup>21</sup>F. Herman and S. Skillman, *Atomic Structure Calculations* (Prentice-Hall, New York, 1963).
- <sup>22</sup>B. F. J. Luyken, F. J. de Heer, and R. Ch. Baas, *Physica (Utr.)* **61**, 200 (1972).
- <sup>23</sup>D. P. Spears, H. J. Fishbeck, and T. A. Carlson, *Phys. Rev. A* **9**, 1603 (1974).
- <sup>24</sup>L. Minnhagen, H. Strihed, and B. Petersson, *Ark. Fys.* **39**, 471 (1969).
- <sup>25</sup>B. F. J. Luyken, *Physica (Utr.)* **60**, 432 (1972).
- <sup>26</sup>K. Siegbahn, C. Nordling, G. Johansson, J. Hedman, P. F. Hedén, K. Hamrin, U. Gelius, T. Bergmark, L. O. Werme, R. Manne, and Y. Baer, *ESCA Applied to Free Molecules* (North-Holland, Amsterdam, 1969).
- <sup>27</sup>I. E. McCarthy, A. Ugbabe, E. Weigold, and P. J. O. Teubner, *Phys. Rev. Lett.* **33**, 459 (1974).